ACS OMEGA

http://pubs.acs.org/journal/acsodf

Article

# Detecting Differences in Prion Protein Conformation by Quantifying Methionine Oxidation

Christopher J. Silva* and Melissa Erickson-Beltran

Cite This: *ACS Omega* 2022, 7, 2649−2660

Read Online

ACCESS | Metrics & More | Article Recommendations | Supporting Information

**ABSTRACT:** A prion's pathogenic character is enciphered in its conformation, which also defines the chemical environments of its amino acids. Differences in chemical environments influence the reactivity of amino acid side chains, in a conformation-dependent manner. Chemical oxidation of susceptible methionines would identify those methionines on the surface of a prion, which would reveal conformation-dependent information. We identified a set of methionine-containing peptides derived from the tryptic, chymotryptic, or tryptic/chymotryptic digestion of recombinant prion protein and the Sc237 strain of hamster-adapted scrapie. We developed a multiple reaction monitoring-based method of quantifying the extent of the methionine oxidation in those peptides. This approach can be used to define a prion's conformation and to distinguish among prion strains, which is an important component of food safety.

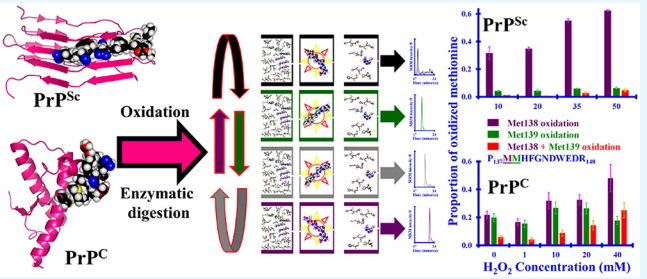


## INTRODUCTION

Prions ($PrP^{Sc}$) are pathological proteins that amplify by inducing a natively expressed prion protein ($PrP^{C}$) to adopt the prion conformation.[1,2] Extensive mass spectrometry-based analysis has shown no covalent differences between $PrP^{C}$ and $PrP^{Sc}$.[3,4] The only demonstrated difference between the two isoforms is their conformation. $PrP^{C}$ is a monomer, whose secondary structure has been characterized by nuclear magnetic resonance and X-ray-based analysis and shown to be composed of $\alpha$-helix, random coil, and a small amount of $\beta$-sheet.[5,6] In contrast, $PrP^{Sc}$ is a poorly characterized multimer composed mostly of $\beta$-sheet and random coil, based on hydrogen-deuterium exchange mass spectrometry and Fourier transform infrared spectroscopy.[7,8] The $PrP^{C}$ monomer shows no special resistance to digestion by proteinase K (PK), while $PrP^{Sc}$ shows significant resistance to PK digestion.[2]

A prion's pathologic character resides solely in its conformation, which means that this property is lost once $PrP^{Sc}$ is inactivated by the denaturation required for mass spectrometry-based analysis.[2,9] The chemical environment of an amino acid is determined by the conformation of the protein in which it is contained, which means that the same amino acid can react differently with an identical reagent, in a conformation-dependent manner. Fortunately, the conformational differences in proteins can be captured by covalent modification.[4,10−14] The covalent differences are imparted by PK digestion, where PK will completely digest $PrP^{C}$ but only partially digest $PrP^{Sc}$ to yield an infectious and characteristic truncated protein, PrP 27−30.[15] Differences in the reactivity of lysines with acylating reagents have been used to detect $PrP^{Sc}$ in the presence of $PrP^{C}$ and to distinguish among prion conformations.[10,11] Acylation leaves the prion's infectivity largely intact.[16] Diethyl pyrocarbonate reacts with the histidines in purified $PrP^{Sc}$ to yield the corresponding ethoxyformyl adducts and a consequent 1000-fold reduction of infectivity.[17] The loss of infectivity can be restored when the ethoxyformyl group is removed from the ethoxyformylated histidines.[17] In this way, covalent modification of prions can yield useful structural information.

Prion protein (PrP) contains more methionines than are typical of a mammalian protein, and those methionines are susceptible to oxidation by selected reagents.[18] Oxidized methionine was proposed to be a covalent signature of prions but has since been shown to be an artifact.[4,19] Oxidizing reagents have been used to study the role of methionine in PrP.[20,21] Mammals possess two generic methionine sulfoxide reductases (Msr A and Msr B) to maintain the methionines in a naturally reduced state.[22] It has been proposed that these methionine reductases are part of a general cellular mechanism of scavenging reactive oxidized species.[23] Other studies of specific methionine oxidation have shown that the methionine oxidation in $PrP^{Sc}$ is consistent with artifactual oxidation.[4,12,24] After extensive oxidation, prions remain infectious, which

**Received:** September 9, 2021
**Accepted:** December 24, 2021
**Published:** January 7, 2022

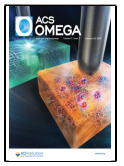





https://doi.org/10.1021/acsomega.1c04989
*ACS Omega* 2022, 7, 2649−2660

indicates that oxidation of a prion's methionines does not substantially alter its structure.[25]

Specific methionines play a crucial role in prion propagation. Humans homozygous for methionine at position 129 were found to be the most susceptible to and had the shortest disease course for the acquired human prion disease Kuru.[26,27] Almost all of the patients afflicted with variant Creutzfeldt-Jakob disease, the human manifestation of cattle-derived bovine spongiform encephalopathy, were homozygous for methionine at position 129.[28] The course of other human familial prion diseases is influenced by methionine at position 129.[29] Chronic wasting disease (CWD) progresses most rapidly in animals homozygous for methionine at position 132, which is isosequential to position 129 in humans.[30] Unlike lysine or histidine, methionine is nonpolar. Methionines may reside in nonpolar regions of a protein that make oxidation by charged species difficult. In addition, other amino acids may influence the extent of methionine oxidation.[12] The structure of $PrP^{Sc}$ makes it difficult to repair with MsrA and MsrB.[31]

We developed methods to analyze methionine-containing peptides from PrP. The peptides were optimized for a multiple reaction monitoring (MRM) method. Chromatographic conditions were developed to separate the oxidized and unoxidized peptides. The relative amount of oxidized methionine in each peptide was determined. We report those results below.

## RESULTS

***In Silico* Digestion of Recombinant PrP (rPrP) to Identify Conditions to Isolate Methionine-Containing Peptides.** The numbering systems used in this paper are for the mature sheep (25−233) or hamster (23−231) normal cellular prion protein (Figures S1 and S2). A partial list of species possessing the peptide sequences in this manuscript has been tabulated (Table S3). For example, methionine at position 132 in sheep and other species is equivalent to methionine 129 in hamsters and humans. The methionine-containing peptides used in this study are derived from the digestion of hamster rPrP or $PrP^{Sc}$ with trypsin to yield PMMHFGNDWEDR (hamster; positions 137−148), IMER (hamster; positions 205−208), and VVEQMCTTQYQK (hamster; positions 209−220). We also used seven synthetic polymorphic chymotryptic peptides (Table S3), MLGS**A**M**S**RP**L** (sheep and other species; positions 132−141) MLGS**A**M**N**RP**L** (sheep and other species; positions 132−141), MLGS**V**MS**R**P**L** (sheep and other species; positions 132−141), MLGS**A**M**S**RP**F** (sheep; positions 132−141), MLGS**A**M**S**RP**I**, (human and other species; positions 129−138), Y**H**ENMY (sheep and goat; positions 153−158), and Y**R**ENMY (sheep and other species; positions 153−158), In addition, a synthetic peptide, MLGSAMSR (hamster and other species; positions 129−136 [hamster numbering]), that could be derived from the sequential tryptic/chymotryptic digestion of sheep or hamster PrP, was also evaluated. These peptides were optimized for MRM-based analysis (Figure S3). The MRM transitions for these ions were empirically determined. The optimized transitions were used to detect and distinguish among these various oxidized methionine-containing peptides.

MRM optimization was based on the fragmentation of the peptides into characteristic ions, which can be used to identify oxidized peptides and the oxidized methionine. The most intense ion of the MLGS**X**M**X′**RP**X″** (**X** = A or V; **X′** = S or N; **X″** = L, F, or I) peptides is the y8 ion, GS**X**M**X′**RP**X″** (Figure S4). By measuring the y8 ion (GS**X**M**X′**RP**X″**) and the parent ion (MLGS**X**M**X′**RP**X″**), the specific oxidized methionine can be identified. If the initial methionine (position 132) is oxidized, then the molecular weight of the parent ion will be increased by 16, but the molecular weight of the y8 ion will remain the same. If the other methionine (position 137) is oxidized, then both the parent ion and the y8 ions will be increased by 16. If methionine 132 and 137 are both oxidized, then the parent ion will be increased by 32 and the y8 ion will be increased by 16. The oxidized peptides are readily separated by chromatography (Figure S5). The y6 (GSAMSR) ion is the most intense ion from the fragmentation of the tryptic/chymotryptic peptide, MLGSAMSR (hamster; positions 129−136). An analogous method of analysis can be used to quantify the oxidation of the methionines of the MLGSAMSR peptide. These oxidized species are also readily separated by chromatography (Figure S6). In this way, the amount and locations of methionine oxidation can be identified in these peptides.

The other two methionine-containing peptides can be analyzed in a similar fashion. The tryptic hamster peptide, PMMHFGNDWEDR (hamster; positions 137−148), could be analyzed using the y3 ion. This transition permits us to distinguish among the oxidized methionines by filtering the +16 or +32 parent ions and then detecting the y3 ions. Chromatography was used to separate the unoxidized, each of the singly oxidized, and the doubly oxidized peptides (Figure S6). The chromatographic retention time of the parent ion to the a2 ion (PM) transition was used to distinguish among the two mono-oxidized peptides. In this way, the extent of methionine oxidation in two-methionine-containing peptides can be analyzed.

Peptides containing a single methionine can be analyzed using the fragmentation of the parent into daughter ions. The oxidation of the hamster-derived tryptic peptides VVEQMCTTQYQK (hamster; positions 209−220) and IMER (hamster; positions 205−208) can be analyzed using the transition of the parent ion to the a2 or y3 ions, respectively. The chymotryptic peptides, Y**H**ENMY (sheep and goat; positions 153−158) and Y**R**ENMY (sheep and other species; positions 153−158), can be analyzed using the parent ion to the respective b5 transitions. The IMER, Y**H**ENMY, and Y**R**ENMY peptides contain a single methionine or oxidized methionine which are readily separated (Figure S7). The chromatographic separation of the oxidized and unoxidized VVEQMCTTQYQK peptides has been previously reported.[4] These physicochemical properties permit the analysis of these methionine-containing peptides.

**Air Oxidation of Methionine-Containing Peptides.** The chemistry of MLGS**X**M**X′**RP**X″** (**X** = A or V; **X′** = S or N; **X″** = L, F, or I) peptide air oxidation was analyzed using the described MRM (*vide supra*) method. The peptides were dissolved in buffer and agitated at 37 °C to allow for air oxidation of the peptide's methionines. Samples were periodically removed for analysis. The signals from these time courses were integrated and are summarized in Figure 1. The MLGS**X**M**X′**RP**X″** (**X** = A or V; **X′** = S or N; **X″** = L, F, or I) peptides differ in the relative oxidation of the methionines at positions (sheep numbering) 132 (Met132) and 137 (Met137). An analogous experiment was performed with the MLGSAMSR peptide, and the results are summarized in


https://doi.org/10.1021/acsomega.1c04989
ACS Omega 2022, 7, 2649−2660

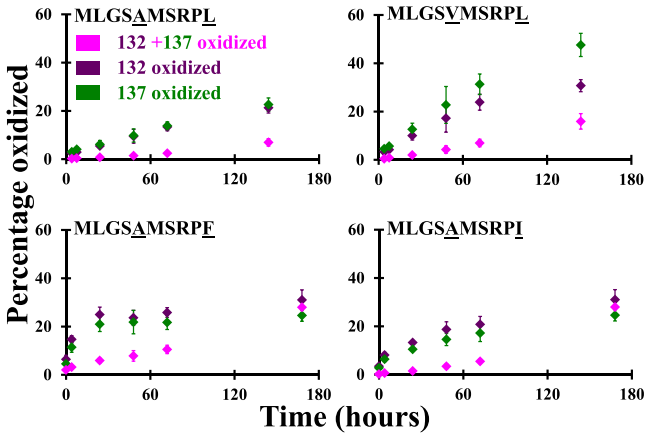


**Figure 1.** Percentage of methionines oxidized in four peptides [MLGSAMSRPL (sheep and other species; positions 132−141), MLGSVMSRPL (sheep and other species; positions 132−141), MLGSAMSRPF (sheep; positions 132−141), and MLGSAMSRPI (human and other species; positions 129−138)] over time. The peptides were dissolved in buffer and shaken at 37 °C. Aliquots were removed at the indicated times and analyzed by MRM. Each data point was done in triplicate and reported as a mean ± standard deviation.

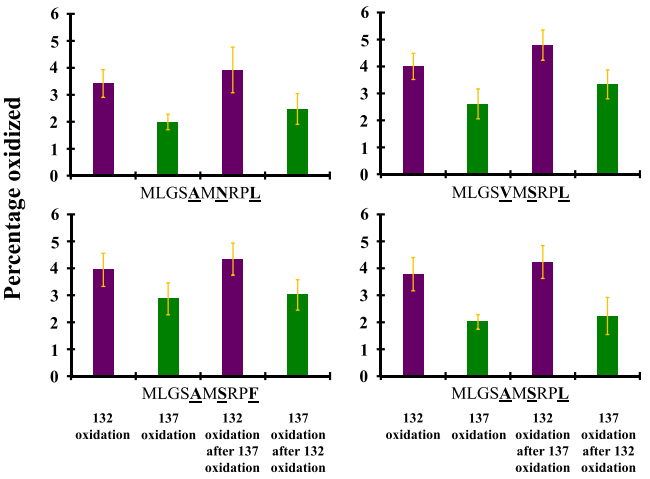


**Figure 2.** Artifactual ESI oxidation of the methionines in four peptides [MLGSAMNRPL, MLGSVMSRPL, MLGSAMSRPF, and MLGSAMSRPL (sheep and other species; positions 132−141)]. The percentage of ESI oxidation of Met132 or Met137 in the unoxidized peptide and that of Met132 or Met137 in a peptide with methionine containing an oxidized Met137 or Met132, respectively, is shown. There was a statistically significant difference ($p < 0.05$) in the greater percentage of oxidized Met132 vs that of Met137, regardless of the oxidation state of the parent peptide. Each data point was done in triplicate and reported as a mean ± standard deviation. Statistical differences were determined by Student's t-test.

Figure S8. This difference in oxidation among these peptides is dependent upon the amino acids in the respective peptides.

Two single methionine-containing chymotryptic peptides, YHENMY and YRENMY, were air-oxidized over time. The differences between the extent of oxidation of the methionine in the YHENMY and YRENMY peptides are dependent upon the amino acids in the peptide, with YHENMY showing more oxidation than YRENMY over time ($p < 0.01$) (Figure S9). Similar results were previously reported for analogues of the VVEQMCTTQYQK peptide.[12] These results indicate that the oxidation of a methionine in a single methionine-containing peptide is influenced by the amino acid composition of that peptide.

**Electrospray Ionization (ESI) Oxidation of Methionine-Containing Peptides.** The oxidative species generated by the process of ESI of the peptides results in their artifactual oxidation.[32,33] The MLGSXMX′RPX″ (X = A or V; X′ = S or N; X″ = L, F, or I) peptides were analyzed by MRM (Figure 2). The signals corresponding to artifactual ESI methionine oxidation have identical retention times to the unoxidized compound yet they appear as peaks in the oxidized transitions. We determined the percentages of artifactual ESI oxidation of Met132 and Met137 (sheep numbering) in the unoxidized peptides. Additionally, we determined the percentage of artifactual ESI Met132 oxidation occurring in peptides containing an oxidized Met137. Conversely, we determined the extent of artifactual ESI Met137 oxidation in peptides containing an oxidized Met132. In the tested unoxidized peptides, Met132 was more susceptible to ESI oxidation than Met137 ($p < 0.01$). In the partially oxidized peptides (Met137 or Met132 oxidized), Met132 ESI oxidation was similarly favored over Met137 oxidation ($p < 0.01$). This indicates that oxidation of one methionine is not dependent upon the oxidative state of the other methionine in the parent ion.

**Chymotrypsin Digestion of Methionine-Containing Peptides.** Oxidation of methionine converts a nonpolar amino acid into a polar one. For comparison, the dipole moment of dimethyl sulfide is 1.5, while that of its oxidized analogue, dimethyl sulfoxide, is 3.6. Chymotrypsin's preference is to cleave on the carboxyl terminus of a nonpolar amino acid. Two chymotryptic peptides, MLGSAMSRPL and MLGSVMSRPL, were digested with chymotrypsin for 0, 30, 60, 120, or 240 min. The samples were analyzed by MRM-based analysis. The percentage of the remaining peptide with Met132, Met137, or Met132 plus Met137 oxidation was determined. The MRM signals were integrated and plotted. The results are summarized in Figures S10 and S11. Extended chymotrypsin digestion does not significantly alter the percentage of Met132 oxidation in the peptide. The percentage of the peptide with Met132 and Met137 oxidation is not significantly altered over the course of the digestion with chymotrypsin.

The percentage of Met137 oxidation increases over the course of the digestion. This suggests that chymotrypsin preferentially cleaves unoxidized Met137 compared to oxidized Met137. Furthermore, there is a significant difference ($p < 0.05$) in the percentage of the Met137 oxidized peptide after 30 min of chymotryptic digestion. Such a preference is not an important consideration when quantifying the total amount of peptide. However, it is significant when the specific purpose is to quantify the extent of methionine oxidation.

The MLGSAMSR peptide is derived from an extended tryptic digestion followed by a short chymotryptic digestion. This peptide was digested with chymotrypsin for 0, 30, 60, 120, or 240 min. The resulting MLGSAMSR peptides (oxidized and unoxidized) were subjected to an MRM-based analysis. The signals from the oxidized and unoxidized peptides were integrated and graphed. These graphs are summarized in Figure S12. After an extended chymotryptic digestion, the percentage of singly oxidized Met129 (=Met132 in sheep and other species) or doubly oxidized Met129 plus Met134 (=Met137 in sheep and other species) peptides remained similar ($p > 0.21$). However, the percentage of oxidized Met134 increased starting after 30 min ($p < 0.05$). There was


https://doi.org/10.1021/acsomega.1c04989
ACS Omega 2022, 7, 2649−2660

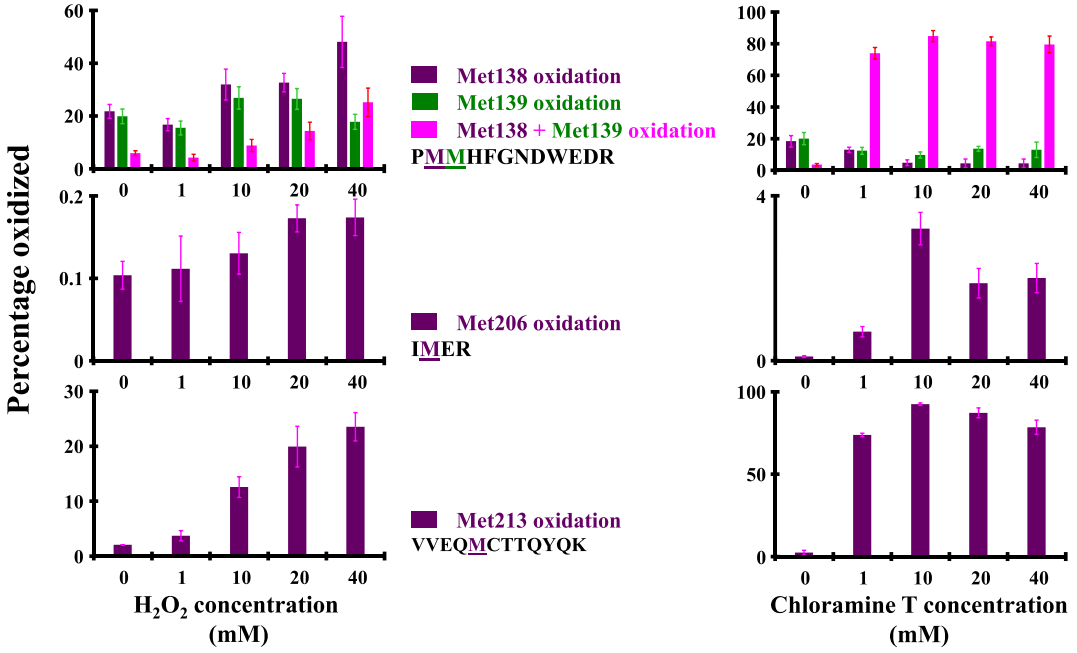


**Figure 3.** Percentage of oxidized methionines present in three hamster tryptic peptides [PMMHFGNDWEDR (positions 137−148), IMER (positions 205−208), and VVEQMCTTQYQK (positions 209−220)] derived from the oxidation of hamster rPrP. rPrP was reacted with one of five different concentrations (0, 1, 10, 20, or 40 mM) of hydrogen peroxide or chloramine T. The reacted rPrP samples were prepared for digestion with trypsin. After the tryptic digestion, the three peptides were analyzed in triplicate by MRM-based mass spectrometry. There was no statistically significant ($p > 0.1$) difference between the percentage of methionine oxidized by hydrogen peroxide at positions 138 and 139 in the PMMHFGNDWEDR peptide at hydrogen peroxide concentrations below 40 mM. At 40 mM, there was a statistically significant difference ($p < 0.05$). Each data point was done in triplicate and reported as a mean ± standard deviation. Statistical differences were determined by Student's t-test.

no difference in the percentage of oxidized Met134 present in the starting (undigested with chymotrypsin) peptide and the same peptide digested with chymotrypsin for 30 min ($p > 0.26$).

**Peroxide Oxidation of rPrP.** Hydrogen peroxide has been widely used to oxidize PrPs. Our MRM method was used to determine that a methionine was oxidized and not another amino acid. Log *P* is a measure of the partitioning of a compound between water and 1-octanol. A smaller number (more negative value) indicates a more hydrophilic molecule. Hydrogen peroxide has a log *P* value of −1.36, which indicates that it will less efficiently oxidize methionines that are in a hydrophobic or surface-inaccessible region of rPrP or $PrP^{Sc}$.

Five different final concentrations of hydrogen peroxide (0, 1, 10, 20, or 40 mM) were reacted with hamster rPrP for 30 min. After the reaction was quenched, the protein was isolated and digested with trypsin. Three tryptic peptides (*vide supra*) were subjected to an MRM-based analysis. The MRM signals were integrated and used to prepare the graphs shown in Figure 3. Again, the observed results show that the extent of oxidation is dependent upon the chemical environment of the methionine. Though these peptides contain a methionine or methionines that will react with an oxidant ($O_2$ or ESI-induced oxidation, vide supra), they react differently with hydrogen peroxide. In addition, the extent of the reaction with hydrogen peroxide is considerably lower than that observed for chloramine T. Again, such differences in reactivity are due to the chemical environment of the methionines of rPrP when they are in the $PrP^{C}$ conformation.

**Chloramine T Oxidation of Hamster rPrP.** Chloramine T is a water-soluble oxidant. It specifically reacts with methionines over other amino acids. Chloramine T has a log *P* value of −1.3. By comparison, oxygen has a log *P* value of 0.65. If a methionine resides in a hydrophobic or surface-inaccessible region of rPrP or $PrP^{Sc}$, then chloramine T may not have access to it.

Hamster rPrP was reacted with five final concentrations (0, 1, 10, 20, or 40 mM) of chloramine T for 30 min. The reactions were quenched, and then the protein was digested with trypsin. Three tryptic peptides, PMMHFGNDWEDR, IMER, and VVEQMCTTQYQK, were selected for analysis. Each was analyzed by our MRM-based method. The integrated results are summarized in Figure 3. These results indicate that even though these peptides contain methionines that react with either molecular oxygen or ESI-generated oxidants, they react differently with chloramine T when they are part of the protein rather than as isolated peptides. These differences in reactivity are due to the chemical environment of the methionines when they are in the rPrP conformation.

**Hydrogen Peroxide Oxidation of the Sc237 Strain of Hamster-Adapted Scrapie.** The Sc237 strain of hamster-adapted scrapie was isolated from the brains of infected hamsters in the terminal stage of the disease. Sc237 prions were isolated by a modified version of the method of Bolton et al.[34,35] The isolated prions were reacted for 30 min with four different final concentrations (10, 20, 35, or 50 mM) of hydrogen peroxide. The reaction was quenched, and the prions were denatured,[36] isolated, and digested with trypsin and then analyzed using our MRM-based analysis. The integrated MRM signals are summarized in the graphs shown in Figure 4. The extent of oxidation of the methionine (Met206) in the IMER peptide is very low, which suggests that it is not surface-exposed. The methionine (Met213) in the VVEQMCTT-QYQK peptide is also less exposed but is comparatively more


https://doi.org/10.1021/acsomega.1c04989
ACS Omega 2022, 7, 2649−2660

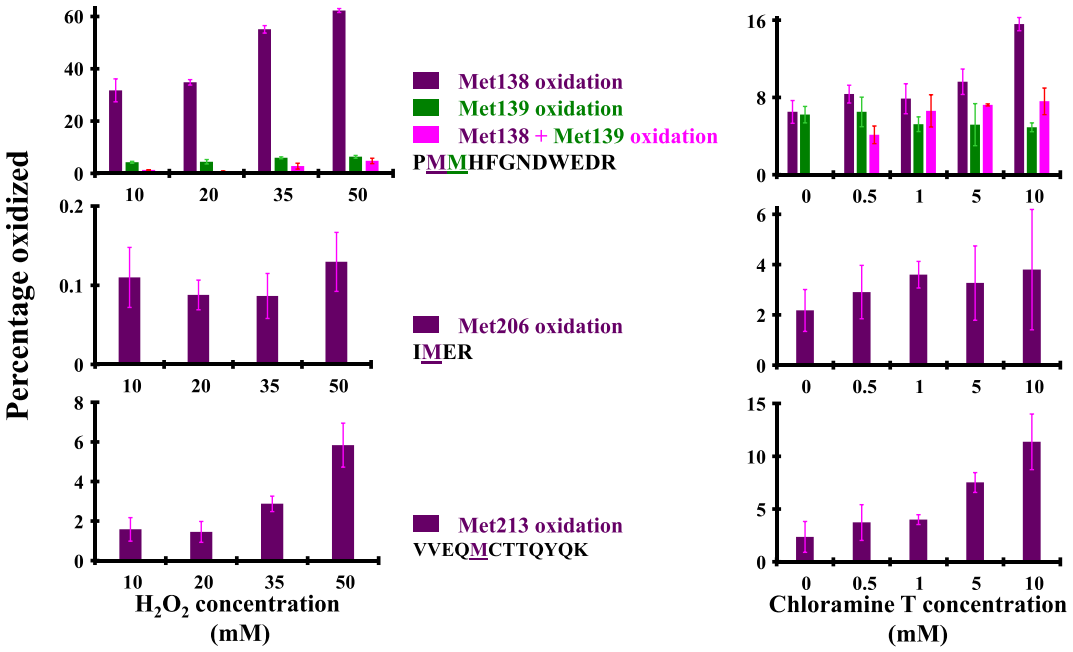


**Figure 4.** Percentage of oxidized methionines present in three hamster tryptic peptides [PMMHFGNDWEDR (positions 137−148), IMER (positions 205−208), and VVEQMCTTQYQK (positions 209−220)] derived from the oxidization of the Sc237 strain of hamster-adapted scrapie. The prions were reacted with one of four different concentrations (10, 20, 35, or 50 mM) of hydrogen peroxide or five different concentrations (0, 0.5, 1, 5, or 10 mM) of chloramine T. The reacted Sc237 samples were prepared for digestion with trypsin. After the tryptic digestion, the three peptides were analyzed in triplicate by MRM-based mass spectrometry. There was a statistically significant ($p < 0.01$) difference between the percentage of methionine oxidized by hydrogen peroxide at positions 138 and 139 in the PMMHFGNDWEDR peptide at all hydrogen peroxide concentrations. There were no statistically significant differences between the percentage of methionine oxidation in the IMER peptide at any concentration of hydrogen peroxide or chloramine T. At higher concentrations of hydrogen peroxide (35 and 40 mM) and chloramine T (5 and 10 mM), there were statistically significant ($p < 0.05$) differences in the percentage of methionine oxidized in the VVEQMCTTQYQK peptide compared to lower concentrations of hydrogen peroxide (10 mM) and chloramine T (0 mM). Each data point was done in triplicate and reported as a mean ± standard deviation. Statistical differences were determined by Student's t-test.

surface-exposed than Met206. The first methionine (Met138) of PMMHFGNDWEDR is significantly more oxidized ($p < 0.01$) than the adjacent methionine (Met139). This difference in reactivity is to be expected if this peptide is part of a $\beta$-sheet motif where adjacent amino acids project in opposite perpendicular directions from the plane of the $\beta$-sheet.

**Chloramine T Oxidation of Hamster-Adapted Scrapie Sc237.** Samples of the Sc237 strain of hamster-adapted scrapie were reacted for 15 min with five different final concentrations (0, 0.5, 1, 5, or 10 mM) of chloramine T. Each sample was processed for an MRM-based analysis. The graphical summaries of the integrated MRM signals are summarized in Figure 4. The extent of oxidation of the methionine (Met206) in the IMER peptide is comparatively low. There were no statistical differences ($p > 0.07$) between the amount of oxidized Met206 in the unreacted Sc237 sample and any of those reacted with chloramine T, suggesting that Met206 is not surface-exposed. At higher concentrations (5 and 10 mM) of chloramine T, there were statistically significant differences between the Met213 oxidized samples and the starting material. This suggests that the Met213 of the VVEQMCTTQYQK sequence is more exposed than Met206 of the IMER sequence. The first methionine (Met138) of the PMMHFGNDWEDR peptide was significantly more oxidized ($p < 0.03$) than the adjacent methionine (Met139) at higher concentrations of chloramine T (5 and 10 mM). This suggests that Met138 has a greater surface exposure than Met139.

## DISCUSSION

We developed an MRM-based method of quantitating the oxidation of methionines present in peptides derived from PrP (rPrP or $PrP^{Sc}$). We used peptides found in sheep, hamsters, and other species (Table S3) to determine how susceptible each methionine in those peptides was to oxidation by air and by reactive oxygen species. We observed that the amino acid composition of the peptide influences the reactivity of each methionine. This occurred in chymotryptic peptides with two methionines (MLGS**V**MSRP**L**, MLGS**A**MSRP**L**, MLGS**A**MSRP**F**, and MLGS**A**MSRP**I**). It was observed in the hamster peptide, MLGSAMSR. It was also observed in peptides containing a single methionine (Y**H**ENMY and Y**R**ENMY). Previous work has shown that this is also true for the sheep analogues of the hamster peptide, VVEQMCTTQYQK.[12] In those peptides with two methionines, each methionine reacted differently. The difference in reactivity between the two methionines was statistically significant, but not substantial, except after extended exposure to air oxidation.

ESI is known to artifactually oxidize methionines in peptides. The oxidants created by ESI are peroxides and hydroxyl radicals. We quantitated the extent of ESI oxidation for four chymotryptic peptides (MLGS**V**MSRP**L**, MLGS**A**MSRP**L**, MLGS**A**MSRP**F**, and MLGS**A**MSRP**I**). These peptides showed small, but significant, differences in the extent of artifactual oxidation. In these samples, Met132 was more readily oxidized than Met137. For two of these peptides (MLGS**A**MSRP**L** and MLGS**V**MSRP**L**), this trend was different from that observed for air oxidation. This suggests


https://doi.org/10.1021/acsomega.1c04989
ACS Omega 2022, 7, 2649−2660

that the choice of oxidant may influence the extent of the reaction.

Oxidized methionines can influence the chymotryptic digestion of MRM-suitable chymotryptic peptides. We observed that chymotryptic digestion of synthetic methionine-containing sheep (and other species Table S3) chymotryptic peptides (MLGS**A**MSRPL and MLGS**V**MSRPL) resulted in an increase in the percentage of oxidized Met137, but not Met132, over time. This suggests that oxidized methionine is not as efficiently cleaved as unoxidized methionine by chymotrypsin. Such a bias can complicate the analysis of samples containing oxidized methionine. When the hamster tryptic/chymotryptic peptide, MLGSAMSR, was digested with chymotrypsin, there was no difference in the percentage of oxidized Met129 in the sample during the entire digestion. After 0.5 h of digestion, there was no difference in the percentage of oxidized Met134 present in the sample compared to the starting material. Thus, an extended tryptic digestion followed by a short chymotryptic digestion can solve this bias problem. Furthermore, this approach is not restricted to hamster as digestion of sheep and other species PrP with trypsin/chymotrypsin will likewise yield the MLGSAMSR peptide.

The chemical environment of a protein also influences the reactivity of the methionines. The methionines in the three hamster tryptic peptides are susceptible to oxidation. When hamster rPrP ($PrP^C$ conformation) was oxidized with either hydrogen peroxide or chloramine T, the extent of methionine oxidation in three tryptic peptides was noticeably different. This indicates that Met206 of the IMER peptide resides in a surface-inaccessible or nonpolar region of the protein, which is inaccessible to the polar oxidants (Figure S13). In contrast, the methionines 138, 139, and 213 are less protected in the PMMHFGNDWEDR and VVEQMCTTQYQK peptides, respectively (Figures S14 and S15). This indicates that the chemical environment of a peptide in a protein influences its reactivity.

When the Sc237 strain of hamster-adapted scrapie was oxidized, we noticed a striking difference in reactivity. Other researchers have shown that exposing prions to oxidants that oxidize methionine does not destroy their infectivity.[25] This means that methionine oxidation does not substantially perturb the prion structure. Methionine 206 of the IMER peptide was not oxidized, so it must not be exposed on the surface of the Sc237 prion. Met213 of the VVEQMCTTQYQK peptide was not as oxidized as it was in the rPrP (=$PrP^C$) conformation, which suggests that it has less surface exposure in the Sc237 conformation than in the rPrP conformation. The most striking difference in oxidation occurs in the adjacent methionines 138 and 139 of PMMHFGNDWEDR. Such a difference is predicted by the $\beta$-sheet geometry, where adjacent methionines project in opposite perpendicular directions from the plane of the $\beta$-sheet. None of these differences in oxidation are due to intrinsic differences in the reactivity of these four methionines, as the synthetic peptides containing them all react with oxidants. The differences in reactivity are due to differences in the conformations of hamster $PrP^C$ and $PrP^{Sc}$.

We compared our empirical results with a computational 4-rung-$\beta$-solenoid model of a murine prion.[37] The model is based on the mouse PrP sequence and does not incorporate the glycosylphosphatidylinositol (GPI) anchor nor the asparagine-linked glycosylation. Despite these limitations, the model accounts for the lack of oxidation of methionine 206 of the IMER peptide (Figure S16) and the partial oxidation of Met213 of the VVEQMCTTQYQK peptide (Figure S17). It does not account for the difference in the relative percentage of oxidized methionines 138 and 139 in the PMMHFGNDWEDR peptide, however. The model would predict an opposite result (methionine 139 more oxidized than methionine 138; Figure S18). This difference may be due to the simplicity of the model (without glycosylation or GPI anchor) or the difference in the PrP sequence (mouse vs hamster; Figure S19). Measuring the surface exposure of methionines by measuring their susceptibility to oxidation can be used to inform modelers, so they can refine their existing models of a prion structure.

Recently, cryo-electron microscopy (cryo-EM) was used to determine the structure of the 263 K strain of hamster-adapted scrapie.[38] Unlike the 4-rung-$\beta$-solenoid,[37] this structure is composed of parallel in-register intermolecular $\beta$-sheets (PIRIBS). Furthermore, it is not a computational model; instead, it is based on cryo-EM analysis. A structure based on the PDB coordinates (7LNA) is shown in Figure S20. Based on this image, there is a pore that appears to make the methionine 206 surface-accessible to hydrogen peroxide (Figure S21). In our experiments, this methionine is not oxidized, which suggests that it is not surface-accessible. In the PIRIBS structure, methionine 213 appears to be surface-inaccessible, which is consistent with the low levels of methionine 213 oxidation. Methionines 138 and 139 appear to have some surface access in the PIRIBS structure. In our experiments, methionine 138, but not 139, is surface-accessible. The reasons for these inconsistencies are unclear. The PIRIBS structure is based on the 263 K strain of hamster-adapted scrapie,[39] while our experiments employed a similar Sc237 strain of hamster-adapted scrapie.[40,41] In addition, the PIRIBS structure is based on PK-treated prions that were isolated using dithiothreitol (DTT),[42] while the prions used in our work were not isolated using DTT, nor were they treated with PK. It is also possible that the static PIRIBS structure shown in Figure S20 is more dynamic and the actual surface exposure of methionines is different from that suggested by the static structure. The reasons for these inconsistencies are unclear, and more experiments need to be performed to resolve them.

Our approach is an important means of ensuring the safety of an important food source that is acquired by means that are largely outside of traditional regulatory controls. Wild game meat accounts for approximately 2.5% of the protein consumed in the United States.[43] Most of this meat comes from cervids (deer, elk, and moose) and is not subjected to regulatory inspection.[44] This is important because CWD,[45] a prion disease of wild and farmed cervids, is becoming more prevalent in North America (https://www.usgs.gov/centers/nwhc/science/expanding-distribution-chronic-wasting-disease?qt-science_center_objects=0#qt-science_center_objects). Fortunately, none of the strains of North American CWD have been shown to be zoonotic (https://www.cdc.gov/prions/cwd/index.html). The recent independent emergence of at least five novel strains of CWD in Norway[46] suggests that cervid $PrP^C$ can propagate a greater number of prion conformations than previously believed. CWD is difficult to control as it spreads among wild cervids by their natural behaviors and from CWD-contaminated environments. In principle, this method can be used to model the compatibility of human $PrP^C$ with a


https://doi.org/10.1021/acsomega.1c04989
ACS Omega 2022, 7, 2649−2660

novel CWD strain (conformation), and, thereby, identify a potential zoonotic prion. Such information will allow regulators to proactively respond. Our approach has the potential to help ensure food safety by identifying potential threats to an important food source that is not subject to regulatory inspection.

## CONCLUSIONS

Our MRM-based method of quantitating oxidized methionine in PrP-derived peptides can be used to distinguish among prion conformations or strains. In the 4-rung-$\beta$-solenoid model, each rung contains at least one methionine per rung (Figure S22). In principle, the surface exposure of a methionine can be used to determine the register (projection inward or outward) for each rung. Previous work has shown that lysine acylating reagents can be used to distinguish among hamster prion strains, as acylation does not eliminate a prion's infectivity.[10,11,14,16] This approach maps the surface of a prion, by quantitating the extent of methionine oxidation. This information can be used to determine the register of each rung on the 4-rung-$\beta$-solenoid and, in principle, distinguish among prion conformations or strains. Such information can be used to model the ability of human $PrP^{C}$ to thread the proposed $PrP^{Sc}$ structure. Thus, covalent modification coupled with mass spectrometry-based analysis can be used to "sequence" a prion's conformation.

## MATERIALS AND METHODS

**Chemicals.** LC/MS-grade acetonitrile, DTT, and water were purchased from Fisher Scientific (Pittsburgh, PA). Chymotrypsin, alpha (3X crystallized zymogen), was purchased from Worthington Biochemical Corporation (Lakewood, NJ). All other reagents were from Sigma-Aldrich (St. Louis, MO).

The peptides used in this study were obtained from Elim Biopharmaceuticals (Hayward, CA). For the sake of clarity, the peptide polymorphisms are underlined and in bold. Mass spectrometry was used to confirm the structures of the synthetic peptides. They are of high (>95%) chemical purity based on LC/UV-based analysis.

Digestion of the appropriate $^{15}$N-labeled rPrP protein with chymotrypsin, trypsin, or a combination of trypsin and chymotrypsin yielded the required $^{15}$N-labeled internal standards. The genetic sequence of the relevant *Prnp* plasmid was used to determine the PrP protein's primary structure. The PrP proteins were analyzed by mass spectrometry to ensure that the predicted amino acid sequences were correct. The incorporation of the $^{15}$N label into the uniformly labeled PrP internal standard was estimated to be 99.7% by mass spectrometry.

**Preparation of Sheep and Hamster rPrP Polymorphisms.** The prion protein genes (sans the N-terminal signal sequence or C-terminal GPI-anchor signal sequence) corresponding to amino acids 25−233 (sheep) or 23−231 (hamster) were cloned using standard protocols into the pET11a vector (EMD Millipore, Billerica, MA). Other polymorphisms were generated using the standard megaprimer method of site-directed mutagenesis.[47,48] Products were checked for correct length by gel, then purified, and digested with NdeI and BamHI and ligated into a pET11a vector (also digested and treated with phosphatase). The ligation mixture (3:1 molar ratio of insert/vector) was transformed into chemically competent DH5$\alpha$ cells (New England Biolabs, Ipswich, MA). The inserts were sequenced with an Applied Biosystems 3130 Genetic Analyzer (Applied Biosystems, Foster City, CA) to verify each mutation. The correctly mutated, sequenced plasmids were isolated and transformed into BL21 cells (EMD Millipore, Billerica, MA) for expression.

**Preparation of $^{15}$N-Labeled Sheep or Hamster rPrP.** Each of the *Prnp*-containing BL21 clones was grown in M9 minimal medium (84.5 mM $Na_2HPO_4$, 44.4 mM $KH_2PO_4$, 17.1 mM NaCl, 37.4 mM $NH_4Cl$, 2 mM $MgSO_4$, 0.1 mM $CaCl_2$, 33.2$\mu$M thiamine, 22.2 mM glucose, and trace metals) supplemented with either naturally abundant $^{14}NH_4Cl$ or $^{15}NH_4Cl$ (99.7% $^{15}$N). Twenty-five mL of the appropriate M9 medium (supplemented with 100 $\mu$g/mL of carbenicillin) in 250 mL flasks was inoculated with a single colony of the desired clone (hamster PrP or sheep PrP with alanine at position 136, arginine at positions 154 and 171 [$A_{136}R_{154}R_{171}$]) and allowed to grow overnight in a shaker/incubator (250 rpm; 37 °C). To minimize isotopic dilution of $^{15}$N, four microliters of the overnight culture grown in M9 medium (+$^{15}NH_4Cl$) was inoculated into a fresh 25 mL culture of M9 medium supplemented with $^{15}NH_4Cl$ and allowed to grow overnight. Four mL of the appropriate overnight culture was added to 150 mL of fresh M9 medium (supplemented with 100 $\mu$g/mL of carbenicillin and $^{15}NH_4Cl$) in a 1 L flask and allowed to grow until the cells achieved midlog growth ($A_{600}$ between 0.4 and 0.6). Once midlog growth was achieved, the cells were induced to overexpress the cloned protein by the addition of a sufficient amount of isopropyl $\beta$-D-1-thiogalactopyranoside (IPTG) to make a 1 mM solution. The cells grew for four more hours. After 4 h, they were pelleted (10,000 × g; 15 min), washed, and then pelleted again. The inclusion bodies were isolated and rPrP purified by previously described methods.[3]

The inclusion bodies from the $^{15}NH_4Cl$ cultures were isolated, denatured, and slowly renatured on an immobilized metal affinity column and then chromatographed on that column. The fraction containing the $^{15}$N-labeled PrP was dialyzed against ammonium acetate (50 mM; pH 4.5) to remove the nonvolatile salts. The retentate was lyophilized to yield a white powder.

The powder was dissolved in buffer (0.01% $\beta$-octylglucopyranoside (BOG), 1 pmol/$\mu$L methionine, and 8% acetonitrile) and then reduced, alkylated, and digested with chymotrypsin. The resulting $^{15}$N-labeled peptides were used as internal standards.

**Preparation of the Naturally Abundant ($^{14}$N)-Labeled rPrP.** The same procedure for preparing $^{15}$N-labeled rPrP was used to prepare naturally abundant ($^{14}$N-labeled) rPrP (*vide supra*), except that the M9 medium was supplemented with naturally abundant $^{14}NH_4Cl$, and the second overnight 25 mL culture was omitted.

**Identification of Peptides via Qualitative Mass Spectrometry.** Qualitative mass spectrometry was performed using a Thermo Scientific, Orbitrap Elite mass spectrometer (Thermo Scientific, Waltham, MA). Synthetic peptides or peptides generated from recombinant proteins digested with trypsin or chymotrypsin were solubilized with 5% acetonitrile, 0.1% formic acid in water (Optima LC/MS grade, Fisher Scientific, Pittsburgh, PA), to approximately 1 pmol/$\mu$L. Each sample was transferred to an autosampler vial and placed in the autosampler of an Eksigent nanoLC 400 interfaced to an Orbitrap Elite mass spectrometer with a PicoChip nanospray


https://doi.org/10.1021/acsomega.1c04989
ACS Omega 2022, 7, 2649−2660

source (New Objective, Woburn, MA). For each LC−MS run, a 2 μL portion of sample was loaded by the autosampler onto a 75 μm ID column containing 10 cm of 3 μm, 120 Å, ReproSil-Pur C18-AQ reverse phase packing (New Objective, Woburn, MA).

Samples were eluted into the mass spectrometer with a binary gradient flow at a rate of 300 nL/min. Solvent A was 2% acetonitrile, 0.1% formic acid in water, and Solvent B was acetonitrile (Optima LC/MS grade containing 0.1% formic acid; Fisher Scientific, Waltham, MA). The gradient was programmed from 5% Solvent B to 50% Solvent B over 30 min, then to 90% solvent B for 20 min, and held at 90% B for 10 min. Peptides were detected in the Orbitrap with the FT survey scan from 300 to 2000 $m/z$ at a resolution of 60,000. The 10 most intense peaks above a threshold of 30,000 counts were subjected to dissociation (CID) with normalized collision energy set to 35, default charge state set to 2, isolation width set to 2.0 $m/z$, and activation time set to 30 ms. Product spectra were recorded at 30,000 resolution with the low mass set to 50 Da. Dynamic exclusion was enabled for a duration of 6 s with a repeat count of 1. Charge state screening allowed +1 and greater charge states to be selected for CID fragmentation. Monoisotopic precursor selection was enabled. MS/MS data were searched against both public and in-house generated databases using the Mascot Server protein identification software (Matrix Science Inc., Boston, MA) to identify peptides of interest.

**Optimization of Peptides.** Peptides were commercially prepared by Elim Biopharmaceuticals (Hayward, CA) for optimization studies. The instrument response was optimized for each peptide by a previously described method.[49] The mass spectrometer was operated in MRM mode, alternating between detection of the oxidized and unoxidized peptides and the $^{15}$N-labeled internal standards. The mass settings for the peptides are summarized in Tables S1 and S2.

**Chymotrypsin Digestion of Peptides.** To test the susceptibility of methionine-containing peptides for further digestion by chymotrypsin, the following peptides were each diluted to 83.3 fmol/μL in chymotrypsin buffer (100 mM Tris pH 8, 10 mM CaCl2): MLGSAMSR (hamster and other species; positions 129−136), MLGS**A**M**S**RP**L** (sheep and other species; positions 132−141), and MLGS**V**M**S**RP**L** (sheep; positions 132−141). For the sake of clarity, the relevant polymorphisms are denoted in bold and underlined. Chymotrypsin was added to a final concentration of 500 ng/100 μL and 500 μL final volume. At each time point (0, 0.5, 1, 2, and 4 h), an aliquot of 100 μL was removed to a new tube, and 2.5 μL of 10% formic acid (Fisher Scientific) was added to each and then filtered through a 10 K molecular weight cut-off (MWCO) filter.

**Air Oxidation of Peptides.** The following peptides were diluted to make a 1 mL solution containing 83.3 fmol/μL of each peptide in 8% acetonitrile. Peptides were subjected to air oxidation in sets. Set 1 contained the peptides MLGS**V**M**S**RP**L** (sheep and other species; positions 132−141), MLGS**A**M**S**RP**F** (sheep and other species; positions 132−141), MLGS**A**M**S**RP**I** (human and other species; positions 129−138), and Y**R**ENMY (sheep and other species; positions 153−158). Set 2 contained the peptides MLGS**A**M**S**RP**L** (sheep and other species; positions 132−141), Y**H**ENMY (sheep and goats; positions 153−158), and MLGS**A**M**N**RP**L** (sheep and other species; positions 132−141). Set 3 contained the three hamster peptides IMER (positions 205−208), PMMHFGNDWEDR (positions 137−148), and MLGSAMSR (positions 129−136).

The solutions were shaken at 500 rpm at 37 °C to permit air oxidation. A 100 μL aliquot (+2.5 μL of 10% FA) of each solution was removed after 0, 4, 24, 48, 72, or 168 h. Each aliquot was filtered through a 10,000 MWCO filter (12 min, 14,000 × g). Samples were diluted with a $^{15}$N-labeled rPrP, chymotrypsin-digested (for sets 1 and 2), or trypsin-digested (for set 3) internal standard immediately before running on the mass spectrometer.

**Animal Handling and Hamster Scrapie Sample Preparation.** The recommendations contained in the Guide for the Care and Use of Laboratory Animals of the National Institutes of Health guided our animal experiments. The protocols governing this work were approved by the Institutional Animal Care and Use Committee of the United States Department of Agriculture, Agricultural Research Service, Albany, CA (Protocol Number: P-10-3). Isoflurane was used to anesthetize the animals prior to all inoculations or euthanizations. A commercial vendor (Charles River Laboratories; Wilmington, MA) supplied the LVG Syrian golden hamsters (*Mesocricetus auratus*).

The Sc237 strain of hamster-adapted scrapie[40,41] was purchased from InPro Biotechnology (South San Francisco, CA). The Sc237 strain was passaged through LVG Syrian golden hamsters (Charles River Laboratories, Wilmington, MA 01887). The initial inoculum was prepared as a 10% homogenate in PBS from the brain of a hamster in the terminal stage of an Sc237 prion infection. Female LVG hamsters (4 weeks old) were anesthetized with isoflurane and then inoculated intracranially (*ic*) with 50 μL of a 10% brain homogenate (~$10^7$ *ic* $ID_{50}$). The inoculated animals were monitored for clinical signs and were humanely euthanized upon the appearance of terminal clinical signs. The brains were surgically removed postmortem. Each brain was stored at −80 °C until it was processed.

$PrP^{Sc}$ was isolated according to the methods of Bolton et al. with some minor modifications.[34] Briefly, a tissue homogenate (10 or 20%) (w/v) from the brain was made using a disposable homogenizer (OMNI International) in homogenization buffer (water- or potassium-free PBS). The brain homogenates were diluted 1:1 with buffer (20% w/v N-lauroylsarcosine, 19 mM sodium phosphate, pH 8.5) and mixed for 15 min at room temperature. The homogenate was then centrifuged for 18 min (16,000 × *g*; 20 °C), in a refrigerated centrifuge (Eppendorf 5810R), to remove large particles. The supernatant was retained. Individual portions of each tissue homogenate (500 μL) were separately diluted to 3 mL with buffer (10% w/v N-Lauroylsarcosine, 9.5 mM sodium phosphate, pH 8.5) and individually transferred to a separate ultracentrifuge tube (4.2 mL, 16 × 38 mm). The contents of the tube were underlaid with 1 mL of 20% w/v sucrose and sealed. The sample in the sealed tube was centrifuged for 75 min at 150,000 × *g* (46,000 rpm, 20 °C) with a floating Noryl spacer in a Beckman 70.1 Ti rotor to obtain an insoluble pellet.

The resulting pellets were immediately brought up in Z buffer (20 mM Tris pH 8.5 containing 0.1% of the zwittergent Z3−14), transferred to screw top microcentrifuge tubes, and sonicated for 4 × 45 s bursts at maximum power using a microplate cup horn sonicator (Misonix 4000). Samples were then reacted with oxidants as described below and finally, denatured by the addition of a 3× volume of 8 M guanidine hydrochloride (GuCl), to achieve a final concentration of 6 M.


https://doi.org/10.1021/acsomega.1c04989
ACS Omega 2022, 7, 2649−2660

Each resulting solution stood for 24 h at room temperature to allow for full denaturation and then was transferred to a clean screw top microcentrifuge tube. Samples were subjected to reduction, alkylation, and enzymatic cleavage (*vide infra*).

**Hydrogen Peroxide Oxidation of rPrP and Hamster Scrapie.** A fresh stock solution of 30% (v/v) aqueous hydrogen peroxide solution was prepared daily. The aqueous dilutions were prepared from the stock solution. Lyophilized hamster rPrP (10 μg) was dissolved in 100 μL of Z buffer (0.1% Z3−14 in 20 mM Tris pH 8.5). To each 100 μL sample was added 10 μL of a dilution of hydrogen peroxide to give final concentrations of 0, 1, 10, 20, or 40 mM $H_2O_2$. Each sample was rotated in a 37 °C incubator for 15 min. Reactions were quenched by the addition of 50 μL of a 355 mM L-methionine solution in water and rotated an additional 15 min. Enough 8 M guanidine hydrochloride (GuCl) was added to yield a 6 M solution. The reacted rPrPs, in 6 M GuCl, were then reduced and alkylated as described below (*Reduction and Alkylation of PrP Samples*).

For hamster scrapie (Sc237), Bolton pellets were prepared from infected brain homogenate, brought up in 100 μL of Z buffer, and sonicated as described above (*Animal Handling and Hamster Scrapie Sample Preparation*). To each sample was added 10 μL of a dilution of hydrogen peroxide to give final concentrations of 0, 0.5, 1, 5, 10, 20, 35, or 50 mM $H_2O_2$. Each sample was rotated in a 37 °C incubator for 15 min. Reactions were stopped by the addition of 50 μL of a 355 mM L-methionine solution. Hamster scrapie samples were denatured with three volumes of 8 M guanidine hydrochloride and left to denature for 24 h. Denatured samples were transferred to clean tubes and were reduced, alkylated, and methanol-precipitated before digestion with trypsin, chymotrypsin, or a combination of the two enzymes, as described below (*vide infra*).

**Chloramine T Oxidation of Hamster rPrP and Hamster-Adapted Scrapie (Sc237).** Chloramine T solutions at 10× concentrations were prepared fresh daily in Z buffer (0.1% Z3−14 in 20 mM Tris pH 8.5), from a 300 mM concentrate in water. Hamster rPrP (10 μg) was dissolved in 90 μL of Z buffer. Fresh chloramine T solution (10 μL) was added to yield a final concentration of 0 (control), 0.1, 0.5, 1, 5, 10, 20, or 40 mM chloramine T per rPrP sample. The solutions were rotated at room temperature for 15 min. After 15 min, the reaction was quenched by an excess of L-methionine (10 μL of a 355 mM solution), and the tubes were rotated for an additional 15 min at room temperature. Enough 8 M guanidine hydrochloride (GuCl) was added to yield a 6 M solution. The reacted rPrPs in 6 M GuCl were then reduced and alkylated as described below (*Reduction and Alkylation of PrP Samples*).

For hamster-adapted scrapie (Sc237), Bolton pellets were prepared from infected brain homogenate, brought up in 90 μL of buffer (0.1% Z3−14 in 20 mM Tris pH 8.5 buffer), and sonicated as described above (*Animal Handling and Hamster Scrapie Sample Preparation*). To each sample was added 10 μL of a dilution of chloramine T to give final concentrations of 0 (control), 0.1, 0.5, 1, 5, or 10 mM. The solutions were rotated at room temperature for 15 min. After 15 min, the reaction was quenched by an excess of L-methionine (10 μL of a 355 mM solution), and the tubes were rotated for an additional 15 min at room temperature. Hamster scrapie samples were denatured with three volumes of 8 M guanidine hydrochloride and left to fully denature for 24 h. Denatured samples were transferred to clean tubes and were reduced, alkylated, and digested with trypsin, chymotrypsin, or a combination of the two enzymes, as described below (*vide infra*).

**Reduction and Alkylation of PrP Samples.** Each 10 μg aliquot of rPrP not reacted with an oxidant was dissolved in 20 μL of buffer (BOG, 1 pmol/μL methionine, and 8% acetonitrile) and sonicated (Cole-Parmer model 8892; Vernon Hills, IL) for 5 min. A 10 μL aliquot of 15 mM DTT in buffer A (25 mM ammonium bicarbonate (ABC), BOG, 1 pmol/μL methionine, and 8% acetonitrile; pH 8) was added to the sonicated solution and reacted for 1 h (37 °C), with 5 min of sonication every 20 min. The reaction mixture was cooled to room temperature, and then 40 μL of iodoacetamide (IA) buffer (22 mM iodoacetamide in buffer A) was added to the mixture and left to react in the dark at room temperature for 1 h. Any excess IA was quenched by the addition of 20 μL of DTT buffer (22 mM DTT in buffer A). The reduced and alkylated rPrP was enzymatically digested with either trypsin or chymotrypsin as described below.

rPrP samples reacted with oxidants, and hamster scrapie (strain Sc237) samples reacted with oxidants, were reduced and alkylated in 6 M GuCl. Briefly, samples in GuCl were reduced with 25 mM DTT in 25 mM ABC buffer pH 8.0 for 15 min at 50 °C, with 5 min of sonication at the beginning of the incubation. Samples were then cooled and alkylated with 75 mM iodoacetamide in 25 mM ABC for 45 min at room temperature, in the dark. Excess iodoacetamide was quenched by the addition of 25 mM DTT in 25 mM ABC and then methanol-precipitated as described below.

**Methanol Precipitation of Guanidine Hydrochloride (GuCl) Solutions.** Enough cold methanol (−20 °C) was added to the GuCl-containing solutions to make an 85% (v/v) solution. This solution was stored at −20 °C for 1 h. After the hour had passed, the solution was centrifuged (20,000 × *g*; 20 min; −11 °C). The supernatant was removed and disposed of as chemical waste. The pellet was resuspended in cold (−20 °C) methanol and centrifuged (20,000 × *g*; 20 min; −11 °C). The resulting supernatant was disposed of as chemical waste. The pellet was air-dried for 10 min and then stored at −20 °C until ready for enzymatic digestion.

**Enzymatic Digestions of Reduced and Alkylated PrP Samples.** Trypsin or chymotrypsin was used to digest the reduced and alkylated PrP proteins. Two enzymatic digestions were employed: (1) trypsin digestion for 18 h at 37 °C and (2) chymotrypsin digestion for 0, 0.5, 1, 2, or 4 h at 30 °C. For each trypsin digestion, 1 μg of trypsin was used in 50 mM Tris pH 8.0 buffer, and for chymotrypsin, 500 ng was used per sample, with added $CaCl_2$ to 10 mM, also in 50 mM Tris pH 8.0 buffer. After the digestion was complete, digestion was stopped by the addition of 2.5 μL of 10% formic acid. Each sample was filtered through a 10,000 MWCO filter (VWR International, San Francisco, CA) for 12 min at 14,000 × g. Samples were stored at −20 °C until analyzed by mass spectrometry.

**Quantitative Mass Spectrometry: Nanospray Liquid Chromatography and Tandem Mass Spectroscopy (LC−MS/MS).** An Applied Biosystems (AB Sciex LLC, Framingham, MA) model 4000 Q-Trap instrument equipped with a nanoelectrospray source was used to perform nanospray LC−MS/MS. An aliquot (6 μL) of each digest was loaded onto a C-18 trap cartridge [Acclaim PepMap100, 5 μm, 100 Å, 300 μm (inside diameter) × 5 mm (Dionex, Sunnyvale, CA)]. Salts were washed from the cartridge with an acetic acid/acetonitrile/heptafluorobutyric acid/water solution (0.5/1/


https://doi.org/10.1021/acsomega.1c04989
ACS Omega 2022, 7, 2649−2660

0.02/99). The now salt-free bound peptides were eluted onto a reversed-phase column [Vydac (HiChrom, Lutterworth, U.K.) 238EV5.07515, 75 $\mu$m × 150 mm]. The solvents were delivered with an Applied Biosystems model Tempo nanoflow LC system (ABI/MDS Sciex) with an autosampler, a column switching device, and a nanoflow solvent delivery system. Samples were eluted from the column with a binary gradient (A, 0.5% acetic acid in water, and B, 80% acetonitrile with 0.5% acetic acid). The flow rate was 250 nL/min with a 16 min linear gradient starting with 5% B and ending with 100% B. Elution with 100% B was conducted for 7 min followed by a return to 5% B over 4 min. The eluted samples were sprayed with a noncoated spray tip (FS360-20-10-N-20-C12, New Objective Inc., Woburn, MA) onto the Applied Biosystems source, Model Nanospray II.

The mass spectrometer was operated in MRM mode, alternating between detection of the analyte peptides and their appropriate $^{15}$N-labeled internal standards. The mass settings for the peptides were empirically determined and may be found in the Supporting Information. The mass settings for the quantification were done with the IntelliQuant quantification algorithm using Analyst 1.5 software.

***In Silico* Digestion of rPrP.** The hamster and sheep PrP sequences were digested *in silico* using the PeptideCutter (https://web.expasy.org/peptide_cutter/) feature of the Internet based Expasy software (https://www.expasy.org/). The sophisticated model was used to predict the chymotryptic cleavage sites.

**Safety Considerations.** Acetonitrile and other hazardous chemicals were handled in a dedicated chemical safety hood. The Sc237 strain of hamster-adapted scrapie is infectious and was handled in a dedicated biosafety level 2 (BSL2) laboratory. The Animal and Plant Health Inspection Service (APHIS) of the USDA (www.aphis.usda.gov/permits/) inspected the BSL2 laboratory. The BSL2 procedures used to manipulate the Sc237 strain of hamster-adapted scrapie are outlined in the 5th edition of the CDC's biosafety manual, Biosafety in Microbiological and Biomedical Laboratories.[50] Before removal from the dedicated BSL-2 laboratory, the Sc237 strain of hamster-adapted scrapie was inactivated with 6 M guanidine hydrochloride.[36] Each Sc237-containing solution was thoroughly mixed and then allowed to stand for at least 24 h at room temperature.[36] The inactivated Sc237 prions were transferred to clean fresh tubes and removed from the BSL-2 laboratory. The inactivated prions were digested with proteases and then filtered through a 10,000 MWCO filter, before being subjected to mass spectrometry-based analysis.

## ■ ASSOCIATED CONTENT

### Supporting Information

The Supporting Information is available free of charge at https://pubs.acs.org/doi/10.1021/acsomega.1c04989.

Table of MRM parameters, table of peptide polymorphisms present in mammalian species, sequence of sheep and hamster normal cellular prion protein, MRM method scheme, scheme of peptide fragmentation, chromatograms of oxidized peptides, graphs of peptides oxidized by air over time, graphical analysis of oxidized peptides after time-dependent chymotryptic digestion, images of hamster recombinant PrP showing the locations of peptides (IMER, PMMHFGNDWEDR, or VVEQMCTTQYQK), image of the same peptides in a computational 4-rung $\beta$-solenoid model of murine PrP$^{Sc}$, alignment of the mature murine or hamster PrP$^{C}$, image of the PIRIBS structure of the 263 K strain of hamster-adapted scrapie (PrP$^{Sc}$), image of the surface of the PIRIBS structure (residues 203−226), and image showing the location of methionines (hamster numbering) in the 4-rung $\beta$-solenoid model of murine PrP$^{Sc}$ (PDF)

## ■ AUTHOR INFORMATION


### Corresponding Author

**Christopher J. Silva** − *Produce Safety & Microbiology Research Unit, Western Regional Research Center, United States Department of Agriculture, Agricultural Research Service, Albany, California 94710, United States;* orcid.org/0000-0003-4521-6377; Phone: 510.559.6135; Email: christopher.silva@usda.gov; Fax: 510.559.6429

### Author

**Melissa Erickson-Beltran** − *Produce Safety & Microbiology Research Unit, Western Regional Research Center, United States Department of Agriculture, Agricultural Research Service, Albany, California 94710, United States*

Complete contact information is available at: https://pubs.acs.org/10.1021/acsomega.1c04989


### Notes

The authors declare no competing financial interest.

## ■ ABBREVIATIONS USED

BSE, bovine spongiform encephalopathy; CWD, chronic wasting disease; GPI, glycosylphosphatidylinositol; MRM, multiple reaction monitoring; PrP, prion protein; PrP$^{C}$, natively expressed and noninfectious isoform of the prion protein; PrP$^{Sc}$, infectious isoform of the prion protein; rPrP, recombinant PrP, produced by overexpression in *E. coli*, noninfectious, PrP$^{C}$ conformation; TSE, transmissible spongiform encephalopathy

## ■ REFERENCES


(1) Prusiner, S. B. Novel proteinaceous infectious particles cause scrapie. *Science* **1982**, *216*, 136−144.

(2) Prusiner, S. B. Prions. *Proc. Natl. Acad. Sci. U. S. A.* **1998**, *95*, 13363−13383.

(3) Stahl, N.; Baldwin, M.; Teplow, D. B.; Hood, L. E.; Beavis, R.; Chait, B.; Gibson, B. W.; Burlingame, A. L.; Prusiner, S. B., Cataloging post-translational modifications of the scrapie prion protein by mass spectrometry. In *Prion diseases of humans and animals*, Prusiner, S. B.; Collinge, J.; Powell, J.; Anderton, B., Eds.; Ellis Horwood: New York, 1992, 361−379.

(4) Silva, C. J.; Onisko, B. C.; Dynin, I.; Erickson, M. L.; Vensel, W. H.; Requena, J. R.; Antaki, E. M.; Carter, J. M. Assessing the role of oxidized methionine at position 213 in the formation of prions in hamsters. *Biochemistry* **2010**, *49*, 1854−1861.

(5) Hornemann, S.; Korth, C.; Oesch, B.; Riek, R.; Wider, G.; Wüthrich, K.; Glockshuber, R. Recombinant full-length murine prion protein, mPrP(23-231): purification and spectroscopic characterization. *FEBS Lett.* **1997**, *413*, 277−281.

(6) Riek, R.; Hornemann, S.; Wider, G.; Billeter, M.; Glockshuber, R.; Wüthrich, K. NMR structure of the mouse prion protein domain PrP(121-231). *Nature* **1996**, *382*, 180−182.

(7) Baron, G. S.; Hughson, A. G.; Raymond, G. J.; Offerdahl, D. K.; Barton, K. A.; Raymond, L. D.; Dorward, D. W.; Caughey, B. Effect of glycans and the glycophosphatidylinositol anchor on strain dependent

conformations of scrapie prion protein: improved purifications and infrared spectra. *Biochemistry* **2011**, *50*, 4479−4490.
(8) Smirnovas, V.; Baron, G. S.; Offerdahl, D. K.; Raymond, G. J.; Caughey, B.; Surewicz, W. K. Structural organization of brain-derived mammalian prions examined by hydrogen-deuterium exchange. *Nat. Struct. Mol. Biol.* **2011**, *18*, 504−506.
(9) Onisko, B. C.; Silva, C. J.; Dynin, I.; Erickson, M.; Vensel, W. H.; Hnasko, R.; Requena, J. R.; Carter, J. M. Sensitive, preclinical detection of prions in brain by nanospray liquid chromatography/tandem mass spectrometry. *Rapid Commun. Mass Spectrom.* **2007**, *21*, 4023−4026.
(10) Gong, B.; Ramos, A.; Vázquez-Fernández, E.; Silva, C. J.; Alonso, J.; Liu, Z.; Requena, J. R. Probing structural differences between PrP(C) and PrP(Sc) by surface nitration and acetylation: evidence of conformational change in the C-terminus. *Biochemistry* **2011**, *50*, 4963−4972.
(11) Silva, C. J. Using small molecule reagents to selectively modify epitopes based on their conformation. *Prion* **2012**, *6*, 163−173.
(12) Silva, C. J.; Dynin, I.; Erickson, M. L.; Requena, J. R.; Balachandran, A.; Hui, C.; Onisko, B. C.; Carter, J. M. Oxidation of methionine 216 in sheep and elk prion protein is highly dependent upon the amino acid at position 218 but is not important for prion propagation. *Biochemistry* **2013**, *52*, 2139−2147.
(13) Llorens, F.; Thüne, K.; Schmitz, M.; Ansoleaga, B.; Frau-Méndez, M. A.; Cramm, M.; Tahir, W.; Gotzmann, N.; Berjaoui, S.; Carmona, M.; Silva, C. J.; Fernandez-Vega, I.; José Zarranz, J.; Zerr, I.; Ferrer, I. Identification of new molecular alterations in fatal familial insomnia. *Hum. Mol. Genet.* **2016**, *25*, 2417−2436.
(14) Silva, C. J.; Erickson-Beltran, M. L.; Dynin, I. C. Covalent Surface Modification of Prions: A Mass Spectrometry-Based Means of Detecting Distinctive Structural Features of Prion Strains. *Biochemistry* **2016**, *55*, 894−902.
(15) Silva, C. J.; Vázquez-Fernández, E.; Onisko, B.; Requena, J. R. Proteinase K and the structure of PrPSc: The good, the bad and the ugly. *Virus Res.* **2015**, *207*, 120−126.
(16) Silva, C. J.; Erickson-Beltran, M. L.; Dynin, I. C. Quantifying the Role of Lysine in Prion Replication by Nano-LC Mass Spectrometry and Bioassay. *Front. Bioeng. Biotechnol.* **2020**, *8*, No. 562953.
(17) McKinley, M. P.; Masiarz, F. R.; Prusiner, S. B. Reversible chemical modification of the scrapie agent. *Science* **1981**, *214*, 1259−1261.
(18) Bettinger, J.; Ghaemmaghami, S. Methionine oxidation within the prion protein. *Prion* **2020**, *14*, 193−205.
(19) Canello, T.; Engelstein, R.; Moshel, O.; Xanthopoulos, K.; Juanes, M. E.; Langeveld, J.; Sklaviadis, T.; Gasset, M.; Gabizon, R. Methionine sulfoxides on PrPSc: a prion-specific covalent signature. *Biochemistry* **2008**, *47*, 8866−8873.
(20) Wong, B. S.; Wang, H.; Brown, D. R.; Jones, I. M. Selective oxidation of methionine residues in prion proteins. *Biochem. Biophys. Res. Commun.* **1999**, *259*, 352−355.
(21) Breydo, L.; Bocharova, O. V.; Makarava, N.; Salnikov, V. V.; Anderson, M.; Baskakov, I. V. Methionine oxidation interferes with conversion of the prion protein into the fibrillar proteinase K-resistant conformation. *Biochemistry* **2005**, *44*, 15534−15543.
(22) Lourenço dos Santos, S.; Petropoulos, I.; Friguet, B. The Oxidized Protein Repair Enzymes Methionine Sulfoxide Reductases and Their Roles in Protecting against Oxidative Stress, in Ageing and in Regulating Protein Function. *Antioxidants (Basel)* **2018**, *7*, 191.
(23) Lim, J. M.; Kim, G.; Levine, R. L. Methionine in Proteins: It's Not Just for Protein Initiation Anymore. *Neurochem. Res.* **2019**, *44*, 247−257.
(24) Silva, C. J.; Onisko, B. C.; Dynin, I. C.; Erickson-Beltran, M.; Requena, J. R. Time of Detection of Prions in the Brain by Nanoscale Liquid Chromatography Coupled to Tandem Mass Spectrometry Is Comparable to Animal Bioassay. *J. Agric. Food Chem.* **2021**, *69*, 2279−2286.
(25) Smith, J. D.; Nicholson, E. M.; Foster, G. H.; Greenlee, J. J. Exposure of RML scrapie agent to a sodium percarbonate-based product and sodium dodecyl sulfate renders PrPSc protease sensitive but does not eliminate infectivity. *BMC Vet. Res.* **2013**, *9*, 8.
(26) Cervenakova, L.; Goldfarb, L. G.; Garruto, R.; Lee, H. S.; Gajdusek, D. C.; Brown, P. Phenotype-genotype studies in kuru: implications for new variant Creutzfeldt-Jakob disease. *Proc. Natl. Acad. Sci. U. S. A.* **1998**, *95*, 13239−13241.
(27) Lee, H. S.; Brown, P.; Cervenáková, L.; Garruto, R. M.; Alpers, M. P.; Gajdusek, D. C.; Goldfarb, L. G. Increased susceptibility to Kuru of carriers of the PRNP 129 methionine/methionine genotype. *J. Infect. Dis.* **2001**, *183*, 192−196.
(28) Bishop, M. T.; Hart, P.; Aitchison, L.; Baybutt, H. N.; Plinston, C.; Thomson, V.; Tuzi, N. L.; Head, M. W.; Ironside, J. W.; Will, R. G.; Manson, J. C. Predicting susceptibility and incubation time of human-to-human transmission of vCJD. *Lancet Neurol.* **2006**, *5*, 393−398.
(29) Aguzzi, A. Prion diseases of humans and farm animals: epidemiology, genetics, and pathogenesis. *J. Neurochem.* **2006**, *97*, 1726−1739.
(30) O'Rourke, K. I.; Spraker, T. R.; Zhuang, D.; Greenlee, J. J.; Gidlewski, T. E.; Hamir, A. N. Elk with a long incubation prion disease phenotype have a unique PrPd profile. *Neuroreport* **2007**, *18*, 1935−1938.
(31) Binger, K. J.; Griffin, M. D.; Heinemann, S. H.; Howlett, G. J. Methionine-oxidized amyloid fibrils are poor substrates for human methionine sulfoxide reductases A and B2. *Biochemistry* **2010**, *49*, 2981−2983.
(32) Chen, M.; Cook, K. D. Oxidation artifacts in the electrospray mass spectrometry of Abeta Peptide. *Anal. Chem.* **2007**, *79*, 2031−2036.
(33) Morand, K.; Talbo, G.; Mann, M. Oxidation of peptides during electrospray ionization. *Rapid Commun. Mass Spectrom.* **1993**, *7*, 738−743.
(34) Bolton, D. C.; Rudelli, R. D.; Currie, J. R.; Bendheim, P. E. Copurification of Sp33-37 and scrapie agent from hamster brain prior to detectable histopathology and clinical disease. *J. Gen. Virol.* **1991**, *72*, 2905−2913.
(35) Silva, C. J.; Onisko, B. C.; Dynin, I.; Erickson, M. L.; Requena, J. R.; Carter, J. M. Utility of mass spectrometry in the diagnosis of prion diseases. *Anal. Chem.* **2011**, *83*, 1609−1615.
(36) Prusiner, S. B.; Groth, D.; Serban, A.; Stahl, N.; Gabizon, R. Attempts to restore scrapie prion infectivity after exposure to protein denaturants. *Proc. Natl. Acad. Sci. U. S. A.* **1993**, *90*, 2793−2797.
(37) Spagnolli, G.; Rigoli, M.; Orioli, S.; Sevillano, A. M.; Faccioli, P.; Wille, H.; Biasini, E.; Requena, J. R. Full atomistic model of prion structure and conversion. *PLoS Pathog.* **2019**, *15*, No. e1007864.
(38) Kraus, A.; Hoyt, F.; Schwartz, C. L.; Hansen, B.; Artikis, E.; Hughson, A. G.; Raymond, G. J.; Race, B.; Baron, G. S.; Caughey, B. High-resolution structure and strain comparison of infectious mammalian prions. *Mol. Cell* **2021**, *81*, 4540−4551.e6.
(39) Kimberlin, R. H.; Walker, C. A. Evidence that the transmission of one source of scrapie agent to hamsters involves separation of agent strains from a mixture. *J. Gen. Virol.* **1978**, *39*, 487−496.
(40) Kimberlin, R. H.; Walker, C. Characteristics of a short incubation model of scrapie in the golden hamster. *J. Gen. Virol.* **1977**, *34*, 295−304.
(41) Marsh, R. F.; Kimberlin, R. H. Comparison of scrapie and transmissible mink encephalopathy in hamsters. II. Clinical signs, pathology, and pathogenesis. *J. Infect. Dis.* **1975**, *131*, 104−110.
(42) Raymond, G. J.; Chabry, J., Purification of the pathological isoform of prion protein (PrPSc or PrPres) from transmissible spongiform encephalopathy-affected brain tissue. In *Techniques in Prion Research*, Lehmann, S.; Grassi, J., Eds.; Birkhauser Verlag: Boston, 2004, 16−26.
(43) Johnson, J. L.; Zamzow, B. K.; Taylor, N. T.; Moran, M. D. Reported, U. S. wild game consumption and greenhouse gas emissions savings. *Hum. Dimens. Wildl.* **2021**, *26*, 65−75.
(44) Hedman, H. D.; Varga, C.; Duquette, J.; Novakofski, J.; Mateus-Pinilla, N. E. Food Safety Considerations Related to the


https://doi.org/10.1021/acsomega.1c04989
*ACS Omega* 2022, 7, 2649−2660

Consumption and Handling of Game Meat in North America. *Vet. Sci.* **2020**, *7*, 188.
(45) Williams, E. S.; Young, S. Chronic wasting disease of captive mule deer: a spongiform encephalopathy. *J. Wildl. Dis.* **1980**, *16*, 89−98.
(46) Nonno, R.; di Bari, M. A.; Pirisinu, L.; D'Agostino, C.; Vanni, I.; Chiappini, B.; Marcon, S.; Riccardi, G.; Tran, L.; Vikøren, T.; Våge, J.; Madslien, K.; Mitchell, G.; Telling, G. C.; Benestad, S. L.; Agrimi, U. Studies in bank voles reveal strain differences between chronic wasting disease prions from Norway and North America. *Proc. Natl. Acad. Sci. U. S. A.* **2020**, *117*, 31417−31426.
(47) Barik, S. Site-directed mutagenesis by double polymerase chain reaction. *Mol. Biotechnol.* **1995**, *3*, 1−7.
(48) Xu, Z.; Colosimo, A.; Gruenert, D. C. Site-directed mutagenesis using the megaprimer method. *Methods Mol. Biol.* **2003**, *235*, 203−207.
(49) Onisko, B.; Dynin, I.; Requena, J. R.; Silva, C. J.; Erickson, M.; Carter, J. M. Mass spectrometric detection of attomole amounts of the prion protein by nanoLC/MS/MS. *J. Am. Soc. Mass Spectrom.* **2007**, *18*, 1070−1079.
(50) U.S.-NIH, *Biosafety in Microbioloical and Biomedical Laboratories, 5th Edition*(https://www.cdc.gov/biosafety/publications/bmbl5/bmbl.pdf); Government Printing Office.: Washington, D. C., 2009.



https://doi.org/10.1021/acsomega.1c04989
*ACS Omega* 2022, 7, 2649−2660